

# Experimental Study of the Earth Pressure Distribution on Cylindrical Shafts

Tatiana Tobar<sup>1</sup> and Mohamed A. Meguid<sup>2</sup>

**Abstract:** This paper describes the results from an experimental program that has been conducted to investigate the distribution of earth pressure on a cylindrical wall embedded in granular material and subjected to radial displacement. The model shaft has been designed and built using mechanically adjustable segments to control the magnitude and uniformity of the wall movement during the tests. A series of experiments have been performed, and the progressive changes in earth pressure along the shaft have been continuously measured for different wall displacements. Results indicated a rapid decrease in lateral earth pressure when a small wall movement was introduced. When the wall movement reached about 2.5% of the shaft radius, the earth pressure distribution along the shaft became uniform and independent of any additional wall displacement. The experimental results are also compared with some of the available theoretical solutions, and the applicability of these solutions is then examined. DOI: 10.1061/(ASCE)GT.1943-5606.0000535. © 2011 American Society of Civil Engineers.

**CE Database subject headings:** Shafts; Soft soils; Earth pressure; Retaining structures; Displacement.

**Author keywords:** Vertical shafts; Soft ground; Axisymmetric earth pressure; Physical models; Cylindrical retaining walls.

## Introduction

Experimental investigations on model shafts have been very useful in explaining the soil arching phenomenon and the earth pressure acting on a shaft lining. Several studies (e.g. Walz 1973; Lade et al. 1981; Konig et al. 1991; Fujii et al. 1994; Herten and Pulsfort 1999; Chun and Shin 2006) have been conducted to measure the earth pressure distribution owing to the installation of model shafts in granular material. One of the key challenges in developing a shaft apparatus is to simulate the radial deformation of the lining and the associated soil movement during construction. Some of the previously used physical models and the radial displacement required to reach active condition in each case are summarized in Fig. 1. These experimental studies provided the basis for the development of a new mechanically controlled apparatus that satisfies the axisymmetric configuration and allows for the continuous measurement of the earth pressure acting on the shaft lining. A comprehensive evaluation of the different theoretical and experimental techniques of radial earth pressure calculation on cylindrical shafts is given elsewhere (Tobar and Meguid 2010).

In this study, a mechanically adjustable system that utilizes the full axisymmetric configuration is described. The model shaft system has been used to investigate the radial earth pressure acting on a cylindrical shaft installed in dry sand. The setup allowed the uniform reduction of the shaft diameter while continuously

measuring the radial earth pressure during the wall displacement. The experimental results are also compared with some of the available analytical solutions. It should be emphasized that capturing the complete details of the shaft construction procedure is beyond the scope of this study.

## Experimental Setup

The experimental setup consisted mainly of a rigid concrete tank that contained the instrumented shaft and the soil, in addition to a mechanically driven horizontal auger system located at the base of the tank. A schematic of the test setup is shown in Fig. 2. Details of the main components are given below.

### Concrete Tank

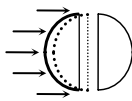
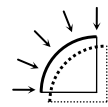
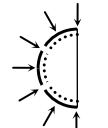
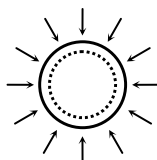
A cylindrical concrete tank is selected for this investigation as it provides the axisymmetric geometry and the rigidity needed to contain the large volume of sand used in the experiment. The concrete tank is 1,220 mm in diameter and 1,070 mm in depth with wall thickness of 127 mm. The interior side of the tank was smoothed and painted to reduce the wall friction (the friction coefficient between the sand and concrete is 0.38). In addition, the tank diameter was chosen to ensure a minimum distance of seven times the shaft radius from the outer perimeter of the shaft to the tank wall. This was considered sufficient to minimize the effect of the rigid boundaries on the measured earth pressures along the shaft. Based on the experimental results of Chun and Shin (2006) as well as Prater's theory (1977), the maximum extent of the failure zone is expected to range from 1 to 3 times the shaft radius, respectively, and therefore no significant lateral pressure is expected from the soil located more than 240 mm from the lining, which is significantly less than the tank radius.

To facilitate the removal of the sand after each test, the tank was equipped with a circular hole (150 mm in diameter) located sideways at the base of the tank. A sand auger powered by an AC motor was used after the completion of the tests to accelerate the sand removal process. The auger system was supported using a

<sup>1</sup>Graduate Student, Dept. of Civil Engineering and Applied Mechanics, McGill Univ., 817 Sherbrooke St. West, Montreal, Quebec, Canada H3A 2K6. E-mail: tatiana.tobarvalencia@mail.mcgill.ca

<sup>2</sup>Associate Professor, Dept. of Civil Engineering and Applied Mechanics, McGill Univ., 817 Sherbrooke St. West, Montreal, Quebec, Canada H3A 2K6 (corresponding author). E-mail: mohamed.meguid@mcgill.ca

Note. This manuscript was submitted on December 5, 2008; approved on March 10, 2011; published online on March 12, 2011. Discussion period open until April 1, 2012; separate discussions must be submitted for individual papers. This technical note is part of the *Journal of Geotechnical and Geoenvironmental Engineering*, Vol. 137, No. 11, November 1, 2011. ©ASCE, ISSN 1090-0241/2011/11-1121-1125/\$25.00.

| Model  | Wall movement required to reach active condition   |
|--|--|
| <br>Semi-cylinder<br>(non-segmented)    | <ul style="list-style-type: none"> <li>Fujii et al. (1994): <math>S \geq 1\% H</math><br/><math>S \geq 6.6\% a</math></li> </ul> |
| <br>Quarter cylinder<br>(non-segmented) | <ul style="list-style-type: none"> <li>Herten &amp; Pulsfort (1999)</li> </ul> $S = 0.05\% H$<br>$S = 0.25\% a$                  |
| <br>Semi-cylinder<br>(Segmented)        | <ul style="list-style-type: none"> <li>Chun &amp; Shin (2006)</li> </ul> $0.6\% H < S < 1.8\% H$<br>$0.15\% a < S < 0.4\% a$     |
| <br>Full cylinder<br>(Segmented)        | <ul style="list-style-type: none"> <li>Present study</li> </ul> $S \geq 0.2\% H$<br>$S \geq 2.5\% a$                             |

**Fig. 1.** Selected physical models used to simulate shaft.  $S$  = radial wall displacement;  $H$  = wall height;  $a$  = shaft radius

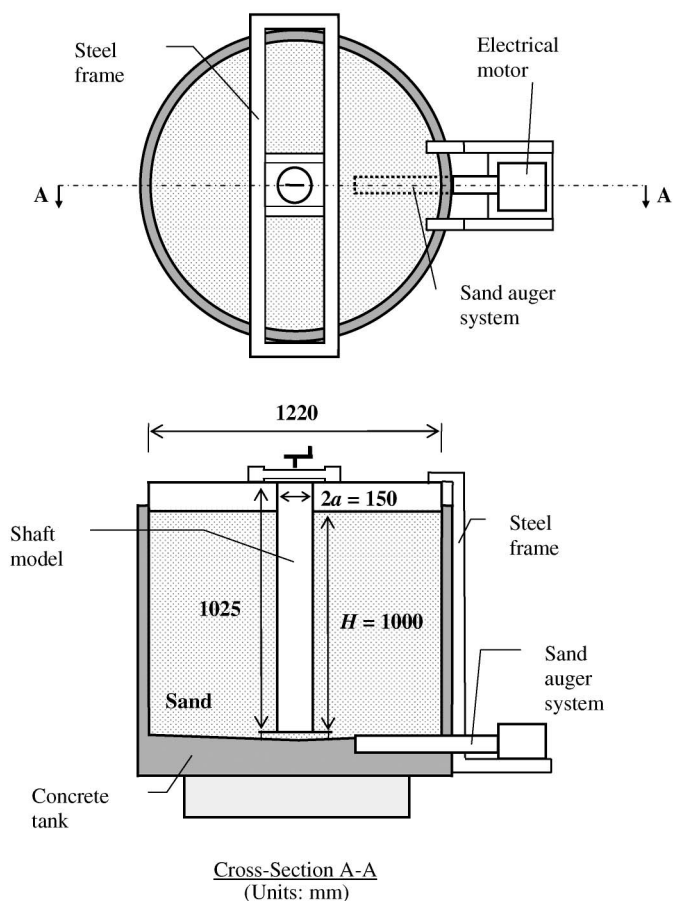


**Fig. 2.** Schematic of the test setup

steel frame located outside the tank and hooked to the tank wall (see Fig. 2).

### Model Shaft

The model shaft consisted mainly of six curved lining segments cut longitudinally from a steel tube with a wall thickness of 6.35 mm (see Fig. 3). The lining segments were machined to fit in segment holders that were attached using steel hinges to hexagonal nuts. These nuts passed through a rod extended through the shaft axis. The axial rod consisted of right-hand and left-hand threaded rods joined by a collar. To contract the diameter of the apparatus, the axial rod is rotated, making the hexagonal nuts move vertically; the nuts, in turn, pull the segment holders radially inward, leading to an inward movement of the lining segments, and consequently, the shaft diameter uniformly decreases.

The lining segments were reinforced using cold-rolled steel strips to increase the rigidity and avoid inward bulging of the lining segments. These strips, along with the segment guide disk and the antirotational rod, prevented rotational movement of the lining segments, keeping them from sliding out of the segment holders. To obtain a uniform horizontal displacement along the lining segments, the steel hinges were assembled at the same angle with the horizontal set by the initial condition disks. Additionally, these disks provided a horizontal sliding guide for the segment holders and a mechanical limit to avoid system overload.

To measure the earth pressure, wall movement, and surface settlement during the test, load cells, displacement transducers, and laser gauge sensors, respectively, were used in the experiments. Three load cells were installed behind one of the lining segments, with sensitive circular areas 1 in. in diameter in contact with the soil. Since the load cells are flushed with the outer shaft surface, the effect of the load cell stiffness on the measured pressure is, therefore, minimized. The centers of these sensitive areas were

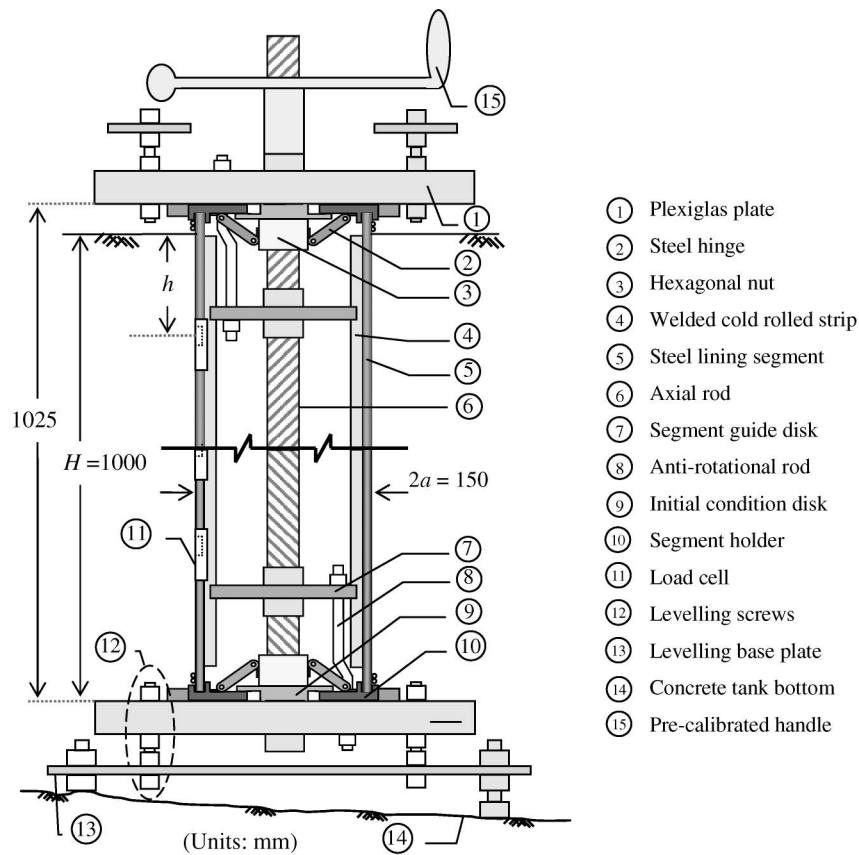


Fig. 3. Vertical cross section of the model shaft

located at distances  $h$  of 84 mm, 240 mm, and 490 mm below the sand surface. A thin plastic film was used to cover the sensitive areas and protect them from the surrounding soil. To ensure that load cells measure the correct pressures, the entire shaft was subjected to hydrostatic pressure, and the readings were recorded and compared to the expected pressure values. Results indicated a linearly increasing pressure with depth with a maximum hydrostatic pressure of 8.7 kPa, which is consistent with the expected value of 8.4 kPa. The cells were also installed on the side of a rigid vertical wall (0.5 m in height and 1 m in length) and subjected to lateral soil pressure induced by coarse sand backfill. The cell readings were consistent with the expected at-rest earth pressure under a two-dimensional condition ( $\gamma h K_0$ ).

Two displacement transducers were used to monitor the wall movement at two locations near the top and bottom of the shaft lining. The transducers were attached to the Plexiglas plates and located horizontally near the ends of the instrumented lining segment. Rigid Plexiglas caps were used to protect the displacement transducers and to ensure proper performance. Two L-Gage-type laser sensors were used to measure the surface settlements at two locations (13 mm and 82 mm) measured from the outer perimeter of the instrumented lining segment.

### Testing Procedure

The first step taken was to prepare the tank and the model shaft, ensuring the cleanness and readiness of the exposed surfaces. The model shaft was installed before sand was rained from a constant height of 1,500 mm above the tank. Coarse sand (Granusil silica

2075, Unimin Corp.) was selected for this study. Sieve analysis, conducted on selected samples, indicated a coarse-grained material ( $D_{10} = 0.75$  mm;  $D_{60} = 1.75$  mm) with no fines. Density cups were placed at different layers inside the tank during the sand placement. The average unit weight across the tank was found to be  $14.7$  kN/m<sup>3</sup>. A summary of the sand properties is given in Table 1. Once the sand reached the target elevation of 1-m-high above the base of the shaft, the sand surface was leveled, and the sand height was checked using the laser sensors to ensure consistent initial conditions for each test. After the initial readings were recorded, the shaft diameter was slowly reduced by rotating the precalibrated handle installed at the top of the shaft and monitoring the readings of the displacement transducers using the data acquisition system. The test was terminated when the maximum displacement reached the target value for each test.

Table 1. Soil Properties

| Property                                   | Value                   |
|--|-------------------------|
| Specific gravity                           | 2.65                    |
| Coefficient of uniformity ( $C_u$ )        | 3.6                     |
| Coefficient of curvature ( $C_c$ )         | 0.82                    |
| Minimum dry unit weight ( $\gamma_{min}$ ) | 14.2 kN/m <sup>3</sup>  |
| Maximum dry unit weight ( $\gamma_{max}$ ) | 16.4 kN/m <sup>3</sup>  |
| Experimental unit weight ( $\gamma_d$ )    | 14.7 kN/m <sup>3</sup>  |
| Soil classification (USCS)                 | Poorly graded sand (SP) |
| Internal friction angle ( $\phi$ )         | 41°                     |
| Cohesion ( $c$ )                           | 0                       |

**Table 2.** Testing Scheme

| Test number | Radial displacement (mm) |
|-------------|--------------------------|
| 1, 2, 3     | 4                        |
| 4, 8, 11    | 3                        |
| 5, 7, 10    | 2                        |
| 6, 9, 12    | 1                        |

### Testing Scheme

The experiments were conducted and repeated three times for each of the four examined wall movements (1, 2, 3, and 4 mm) with a total of 12 tests performed in this study, as summarized in Table 2. The developed testing procedure described above was strictly followed for each test to ensure consistent initial conditions. Selected test results are reported in the following section.

### Experimental Results and Discussion

The earth pressure results presented here are based on load cell readings taken at selected locations along the shaft. Emphasis is placed on the changes in the measured earth pressure before and after a predefined wall movement is induced. The corresponding surface movements are also presented.

#### Active Earth Pressure

The distribution of the measured earth pressure with depth for different wall movements ( $S = 1, 2, 3,$  and  $4$  mm) is shown in Fig. 4. For  $S = 1$  mm, the lateral pressure increased from the surface up to the midheight of the shaft ( $h/a \approx 7$ ), followed by a pressure decrease within the lower half of the shaft. The overall magnitudes of the pressure have decreased by about 60% from the initial values. The lateral pressure further decreased with the increase of wall movement to 2 mm, and the distribution became more uniform with depth, as shown in Fig. 4(b). The additional increase in wall movement to 3 and 4 mm [Figs. 4(c) and 4(d)] did not cause significant changes in earth pressure. To evaluate the performance of some of the available theoretical methods, the experimental results are compared with four different solutions, namely Terzaghi (1943), Berezantzev (1958), Prater (1977), and Cheng and Hu (2005), as shown in Fig. 4.

It was found that the solutions of Terzaghi (1943) and Berezantzev (1958), both assuming a value of  $\lambda$  equal to unity, agree well with the measured earth pressure, provided that enough soil movement is allowed. This is consistent with the fact that Berezantzev's theory is based on the equilibrium of a slipping wedge with failure surface identical to that of Rankine's theory. By comparing the experimental results with the analytical solution of Prater (1977), which is based on Coulomb's wedge analysis under axisymmetric conditions and a value of  $\lambda = K_o$ , it can be seen that the solution computes a zero value of earth pressure at a normalized depth  $h/a$  of about 9 ( $\phi = 41^\circ$  and  $c = 0$ ), which is considered inconsistent with experimental data. Prater suggested the use of the maximum earth pressure value for design purposes. Cheng and Hu (2005) proposed bounds for the earth pressure distribution based on slip line analysis, using different values of the coefficient  $\lambda$ . The upper bound is derived using  $\lambda = K_o$ , whereas the lower bound is derived using  $\lambda = 1$ , which reduces the solution to the one proposed by Berezantzev (1958). As shown in Fig. 4, the calculated pressure distribution for  $\lambda = K_o$  agrees well with the experimental results for the upper half of the shaft when small movements are induced. However, the predicted distribution is

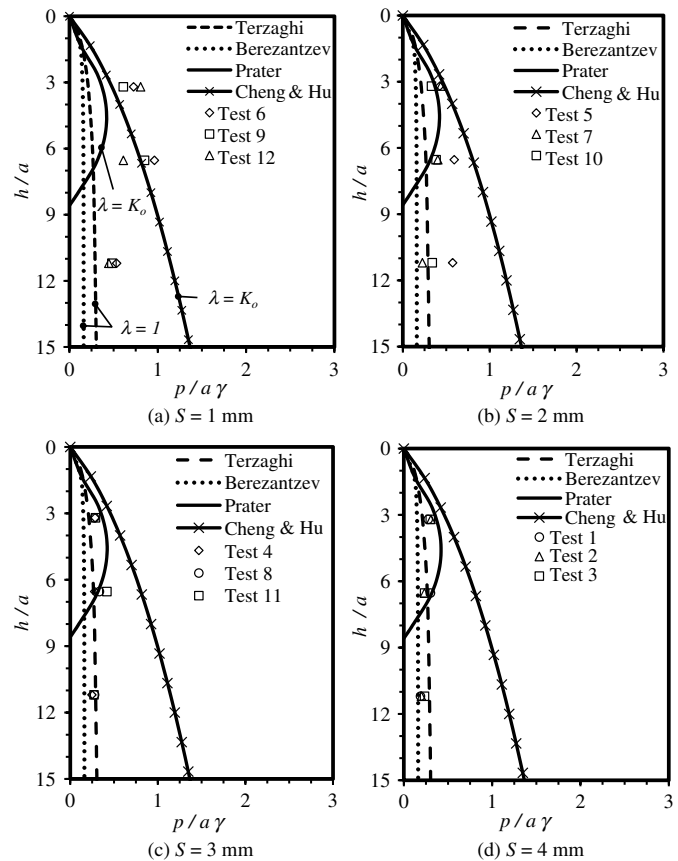


**Fig. 4.** Comparison of measured and theoretical earth pressures along the shaft at (a) 1-mm; (b) 2-mm; (c) 3-mm; and (d) 4-mm wall movement

not uniform and continues to increase with depth. The above comparison highlights the importance of the relationship between the soil movement around the shaft and the expected earth pressure distribution, which has significant implications on the chosen method of analysis.

#### Surface Displacements

The surface settlement was measured at two locations in the close vicinity of the shaft, and the results are summarized in Fig. 5. Surface settlement continued to increase as wall movement increased. For  $r/a = 1.2$ , a maximum settlement of about 8 mm was measured, whereas a settlement of about 5 mm was measured for  $r/a = 2.1$ . This indicates a decreasing settlement with distance

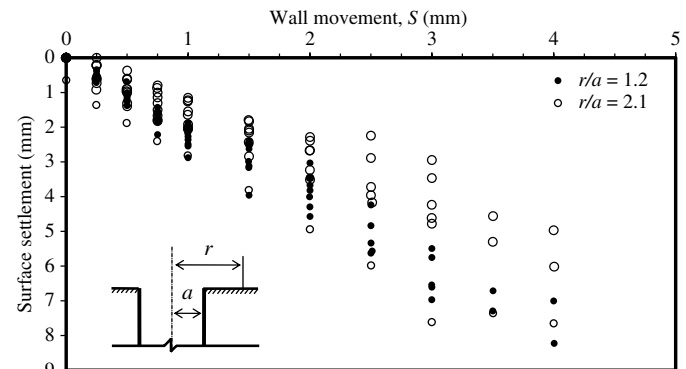


**Fig. 5.** Measured surface settlement

from the shaft. It was also observed, based on the experimental results, that the magnitude of the maximum surface settlement near the shaft circumference ( $r/a = 1.2$ ) was approximately twice the wall movement.

## Summary and Conclusions

An experimental study was performed to investigate the earth pressure distribution on a cylindrical shaft, considering the wall displacement effects. A model shaft was developed to satisfy the full axisymmetric configuration and allow for the continuous measurement of earth pressure for different radial wall movements. The results were compared with some of the available theoretical solutions. For shafts in cohesionless soils, no agreement has been reached among researchers as to the magnitude of wall movement required to reach the active condition. Based on this study, the wall movement needed to establish the active condition (maximum reduction in earth pressure) is approximately 2.5% of the shaft radius, which is equivalent to 0.2% of the wall height. The reduction in earth pressure can reach about 80% of the initial value, in contrast to a reduction of about 40% calculated using  $\gamma h K_a$ .

Both the theoretical and the experimental results showed that the axisymmetric active earth pressure distribution for a cylindrical walls does not increase linearly with depth as it does in long vertical walls under plane strain conditions. As the soil movement increases, the normalized pressure distribution reduces until a constant value (independent of the depth) is reached at the ultimate state. When theoretical solutions are used to calculate the lateral earth pressure on a shaft lining, it is recommended that a coefficient of earth pressure on radial planes ( $\lambda$ ) is chosen such that it ranges between 1 and  $K_o$  to obtain the lower and upper bounds of the pressure distribution, respectively. Full-scale tests are needed to confirm the above experimental findings.

## Acknowledgments

This research is supported by the Natural Sciences and Engineering Research Council of Canada (NSERC) under Grant No. 311971-06. The assistance of Mr. John Bartczak in building the shaft apparatus and conducting the experiments is greatly appreciated.

## Notation

The following symbols are used in this paper:

- $a$  = shaft radius;
- $c$  = soil cohesion;
- $g$  = gravitational constant;
- $H$  = shaft wall height;

- $h$  = excavation depth measured from ground surface;
- $K_a$  = coefficient of earth pressure at active conditions,  $K_a = \tan^2(45 - \phi/2)$ ;
- $K_o$  = coefficient of earth pressure at rest;
- $P = p$  = lateral earth pressure;
- $p_a$  = active earth pressure;
- $P_o$  = lateral earth pressure at  $S = 0$  mm;
- $r$  = radial distance;
- $S$  = radial displacement at shaft wall or radial soil movement at soil-wall interface;
- $\gamma$  = unit weight;
- $\lambda$  = coefficient of lateral earth pressure on radial planes,  $\lambda = \sigma_\theta/\sigma_v$ ;
- $\sigma_r$  = radial stress;
- $\sigma_\theta$  = tangential stress;
- $\sigma_v$  = vertical stress; and
- $\phi$  = angle of internal friction of the soil.

## References

- Berezantzev, V. G. (1958). "Earth pressure on the cylindrical retaining walls." *Proc., Int. Soc. of Soil Mechanics and Foundation Eng. (ISSMFE) Conf. on Earth Pressure Problems*, Butterworths, London, 21–27.
- Cheng, Y. M., and Hu, Y. Y. (2005). "Active earth pressure on circular shaft lining obtained by simplified slip line solution with general tangential stress coefficient." *Chin. J. Geotech. Eng.*, 27(1), 110–115.
- Chun, B., and Shin, Y. (2006). "Active earth pressure acting on the cylindrical retaining wall of a shaft." *South Korea Ground Environ. Eng. J.*, 7(4), 15–24.
- Fujii, T., Hagiwara, T., Ueno, K., and Taguchi, A. (1994). "Experiment and analysis of earth pressure on an axisymmetric shaft in sand." *Proc., 1994 Int. Conf. on Centrifuge*, A. A. Balkema/Rotterdam, Netherlands, 791–796.
- Herten, M., and Pulsfort, M. (1999). "Determination of spatial earth pressure on circular shaft constructions." *Granular Matter*, 2(1), 1–7.
- Konig, D., Guettler, U., and Jessberger, H. L. (1991). "Stress redistributions during tunnel and shaft constructions." *Proc., Int. Conf. Centrifuge 1991*, A. A. Balkema/Rotterdam, Netherlands, 129–135.
- Lade, P. V., Jessberger, H. L., Makowski, E., and Jordan, P. (1981). "Modeling of deep shafts in centrifuge test." *Proc., Int. Conf. on Soil Mechanics and Foundation Engineering*, Vol. 1, Stockholm, Sweden, 683–691.
- Prater, E. G. (1977). "Examination of some theories of earth pressure on shaft linings." *Can. Geotech. J.*, 14(1), 91–106.
- Terzaghi, K. (1943). *Theoretical soil mechanics*, Wiley, New York.
- Tobar, T., and Meguid, M. A. (2010). "Comparative evaluation of methods to determine the earth pressure distribution on cylindrical shafts: A review." *Tunnelling Underground Space Technol.*, 25(2), 188–197.
- Walz, B. (1973). "Left bracket apparatus for measuring the three-dimensional active soil pressure on a round model caisson right bracket." *Baummaschine und Bautechnik*, 20(9), 339–344 (In German).